Observation of $\eta_c(2S)$ in $\psi(2S)\to\gamma K^+K^-\pi^0$

Hu Liu, Liangliang Wang, Yaqian Wang, Ling Yu and Changzheng Yuan

December 20, 2011

Contents

Table 1: Varieties of generated Monte Carlo samples

decay modes	number of events
$\psi' \to \gamma\eta_c(2S), \eta_c(2S) \to K^+K^-\pi^0$	10^5
$\psi' \to \gamma\chi_{c1}, \chi_{c1} \to K^+K^-\pi^0$	10^5
$\psi' \to \gamma\chi_{c2}, \chi_{c2} \to K^+K^-\pi^0$	10^5
$\psi' \to \gamma K^+K^-\pi^0$(PHSP)	10^5
$\psi' \to K^+K^-\pi^0$(via $K^*(892)$)	10^6
$\psi' \to K^+K^-\pi^0\pi^0$(via $K_1(1270)$)	10^6
$\psi' \to$ Neutral+$J/\psi, J/\psi \to \mu^+\mu^-$	10^6
$\psi' \to$ Inclusive	10^8

1 Introduction

The $\psi(2S)$ can decay radiatively to another meson, such as $\chi_{cJ(J=1,2)}$ or $\eta_c(1S)$. However, the radiative decay $\psi(2S) \to \gamma\eta_c(2S)$ has not been observed before, and the decay $\eta_c(2S) \to K^+K^-\pi^0$ final state is just the focus of this analysis.

2 Samples and Software Version

The Software version used in this analysis is BOSS 6.5.1p02(Inclusive MC samples are produced on BOSS 6.5.1). Table 1 shows all the samples used. We use the program LUNDCRM to generate inclusive Monte Carlo (MC) events for background studies. The signal is generated with the corrected angular distribution for $\psi(2S) \to \gamma\eta_c(2S)$, the subsequent $\eta_c(2S) \to KK\pi^0$ decay is generated according to phase space, and π^0 is required to decay fully into γ pair.

3 Event selection

3.1 Selection strategy

The following is the selection of $\gamma K^+K^-\pi^0$ events.

- 2 good charged tracks with net charge zero, and at least 3 good photons.
- good charged (neutral) tracks should both be at the active acceptability of MDC (EMC).
  That's $|\cos\theta| < 0.93$ for charged tracks, $|\cos\theta| < 0.8$ and $0.84 < |\cos\theta| < 0.92$ for photons.
- deposited energy of good photons in EMC must be larger than 25MeV.
- TDC information of good photons in EMC should fall in [0,14] in a unit of 50ns.
- charged tracks are fitted with common VertexFit package to IP (Interaction Point).
- 5-constraints(5C) kinematic fitting are performed on the final state to $\gamma K^+K^-\pi^0$ via looping all those good photons.
  The five constraints are the total energy, the three-dimensional momentum, and the π^0 mass constraint.

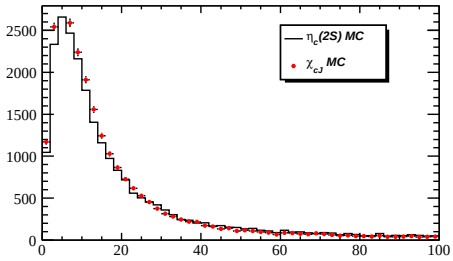

(a) χ^2_{5C} of kinematic fitting

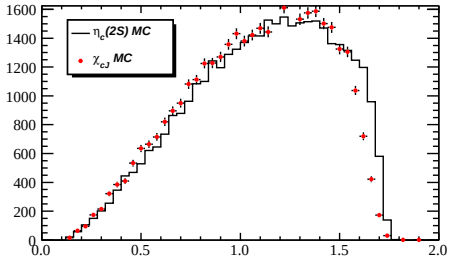

(b) momentum of charged K

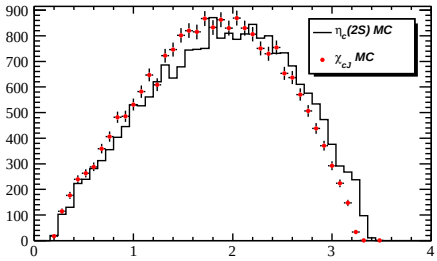

(c) Invariant mass spectrum of the two charged tracks assuming as μ

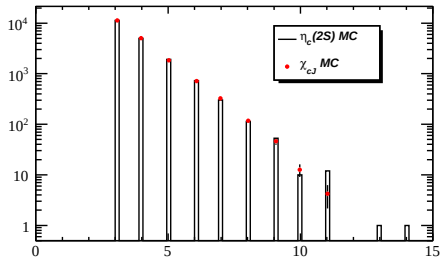

(d) number of Good photons

Figure 1: The comparison of some distributions between $\chi_{cJ(J=1,2)}$ and $\eta_c(2S)$ MC samples, and they agree with each other well. Histogram is $\eta_c(2S)$ MC sample and spot is for $\chi_{cJ(J=1,2)}$.

- Particle ID for charged tracks as Kaon.
  It means, for charged tracks, the probability of Kaon hypothesis is larger than that of any other particles.

3.2 Optimization strategy

The major challenge of this analysis is to detect the low energy ($\sim 50MeV$) transition photon while suppressing serious backgrounds. As a result of this, the study of $\psi(2S) \to \gamma\, \chi_{cJ(J=1,2)}$, $\chi_{cJ(J=1,2)} \to K^+K^-\pi^0$ is carried out to justify the analysis procedures of the $\eta_c(2S)$ analysis.

Finally, the results and systematic uncertainties will be presented.

Fig. 1(a)−Fig. 1(d) show the comparison of some distributions between $\chi_{cJ(J=1,2)}$ and $\eta_c(2S)$ MC samples, and they agree very well. From the comparison, we are confident that it should be reasonable to use $\chi_{cJ(J=1,2)}$ signal for optimization of the $\eta_c(2S)$ signal selection.

4 Background study

4.1 Description of mass spectrum

According to the analysis, one of the main backgrounds in the signal mass region, above $3.6\mathrm{GeV/c^2}$, is $\psi(2S) \to K^+K^-\pi^0$ events. That's due to a fake cluster selected as the real photon. But, if the mass

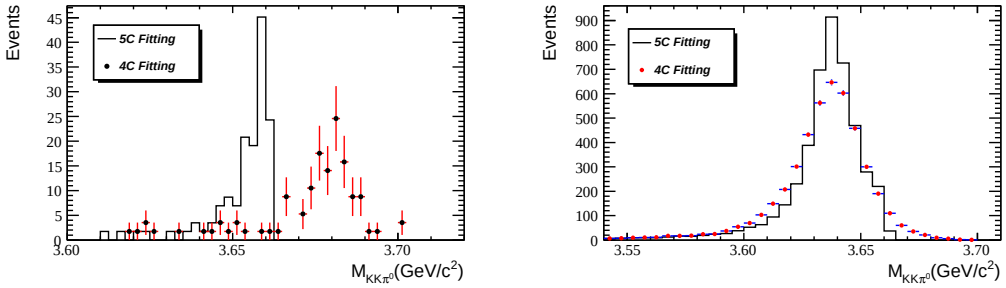

(a) Description of $\psi(2S) \to K^+K^-\pi^0$ Background

(b) Description of Signal $\eta_c(2S)$

Figure 2: Representation of mass spectrum, histogram for 5C and spot for 4C. a) $\psi(2S) \to K^+K^-\pi^0$ background from Inclusive MC sample. b) Signal $\eta_c(2S)$ MC sample.

spectrum is calculated from 4C kinematic fitting, that means the measured energy of the radiative photon is not used, the $K^+K^-\pi^0$ invariant mass of these background events will move upwards like Fig.2(a) shows.

However, from Fig.2(b) we can see there seems little difference for signal mass spectrum between 4C and 5C.

To be more intuitional, we plot these two toghter after 4C and 5C with a reasonable normalization (in fact, which are just scaled to the fitting numbers of corresponding events from data sample.) as Fig.3(a)−Fig.3(d) show. Obviously, a superiority of 4C kinematic fitting can be seen from the pictorial diagram.

4.2 Background from J/ψ related events

The leading decay modes of J/ψ related background are $\psi(2S) \to Neutral + J/\psi$, J/ψ to electron, muon and Kaon pair. In order to suppress these events, we require that the invariant mass of the two charged tracks assuming as muons must be less than $2.9\mathrm{GeV/c^2}$. Fig. 4 shows this distribution (without PID requirements).

4.3 Background from the same final state particles

As we all know, the decay $\psi(2S) \to \omega KK$, $\omega \to \gamma\pi^0$ has the same final state particles with our signal. In order to estimate how much these "the same" events influence our signal region, we require the invariant mass of three photon candidates fall in [0.74,0.82]$\mathrm{GeV/c^2}$, that includes nearly all those ωKK events in data, then we find almost no event exists above $3.6\mathrm{GeV/c^2}$ on $K^+K^-\pi^0$ mass spectrum.

So as to get the corresponding number of such background events while we fit the $\pi^0 KK$ mass spectrum, we directly measure M_ω of those survived events falling in the fitting mass region using the histogram of M_ω from ωKK MC sample with an additional Chebyshev polynomial as PDF like Fig. 5(a) shows.

As said above, those ωKK background events can hardly influence above $3.6\mathrm{GeV/c^2}$ as well as it has a tiny statistic, we arbitrarily apply the lineshape of this background just from MC sample, and the lineshape is simply like Fig. 5(b) shows, which is fitted with a double-Gaussion PDF.

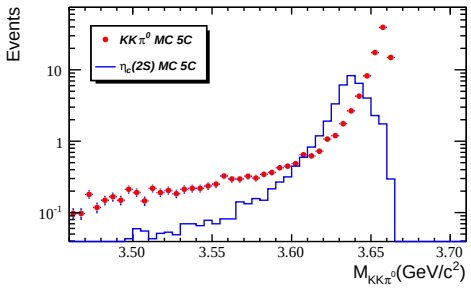

(a) 5C mass spectrum (respective)

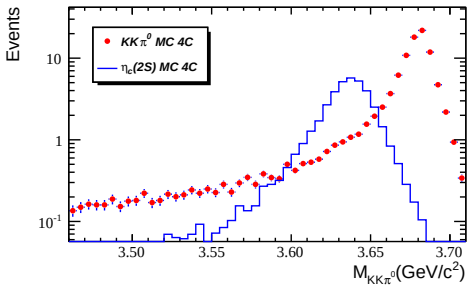

(b) 4C mass spectrum (respective)

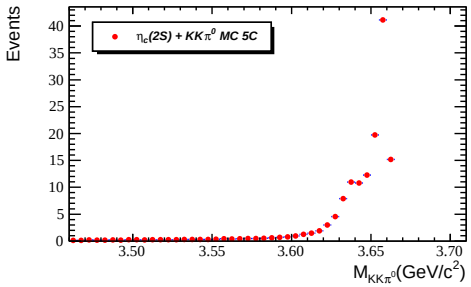

(c) 5C mass spectrum (together)

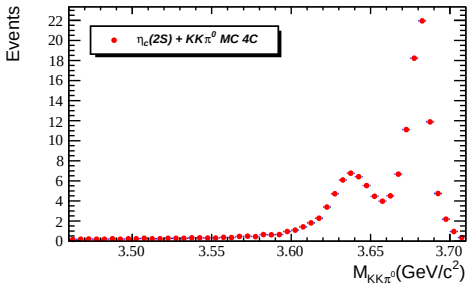

(d) 4C mass spectrum (together)

Figure 3: $\psi(2S) \to K^+K^-\pi^0$ background events can be observably separated from signal $\eta_c(2S)$ events after 4C kinematic fitting. The top two plots are respectively signal $\eta_c(2S)$ and $KK\pi^0$ background events after 4C and 5C. The bottom two show them together with a reasonable normalization.

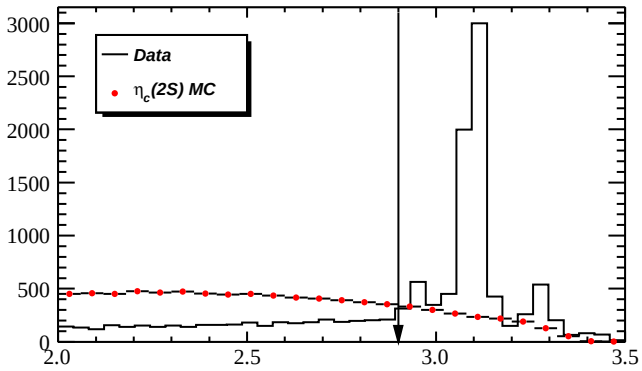

Figure 4: Invariant mass of two charged tracks assuming as μ, spots for signal $\eta_c(2S)$ and histogram for data sample. The three peaks of histogram are respectively $J/\psi \to K^+K^-$, $J/\psi \to e^+e^-/\mu^+\mu^-$, and $\psi(2S) \to \gamma\chi_{c1}$, $\chi_{c1} \to K^+K^-$.

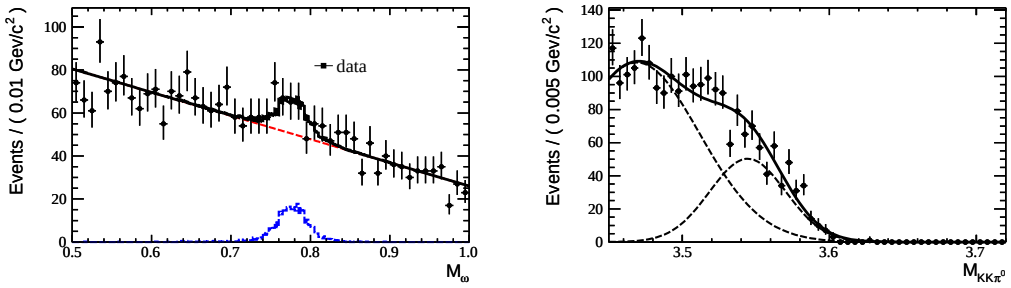

(a) ωKK events inside the fitting mass region in data (b) Lineshape of ωKK background

Figure 5: Fitting of ωKK background events. a) Fitting of M_ω from data sample. b) Lineshape of ωKK events obtained from MC sample (double-Gaussian).

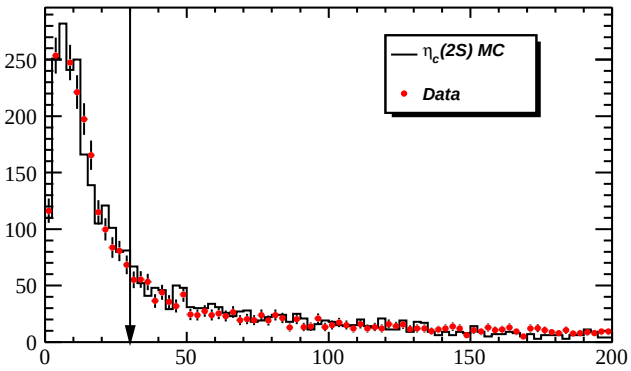

Figure 6: χ^2 of 5C Kinematic Fitting. χ^2_{5C} is required to be less than 30.

4.4 Background from $\pi^0 KK$ and $\pi^0\pi^0 KK$

Now we deal with the background from $\pi^0 KK$ and $\pi^0\pi^0 KK$ events. As explained above, $\pi^0 KK$ events can pollute the $\eta_c(2S)$ mass region with a fake cluster. On the contrary, most $\pi^0\pi^0 KK$ events can survive because one or more real photons is so soft that may not be reconstructed. So as to reduce these background events, we require the χ^2 of 5C kinematic fitting should be less than 30, Fig. 6 shows this distribution.

4.4.1 Lineshape of $\pi^0 KK$

In view of the difference in simulation between data and MC samples, we distinguish $\psi(2S) \to \pi^0 KK$ events into two types, one with Final State Radiation photons (FSR) and the other without (noFSR). Fig. 7(a) and Fig. 7(b) show the $\pi^0 KK$ mass spectrum of these two types of events.

Then we can define a ratio R_{FSR} as follow:

$$R_{FSR} = \frac{N^{MC}_{FSR} * f_{FSR}}{N^{MC}_{noFSR}} \tag{1}$$

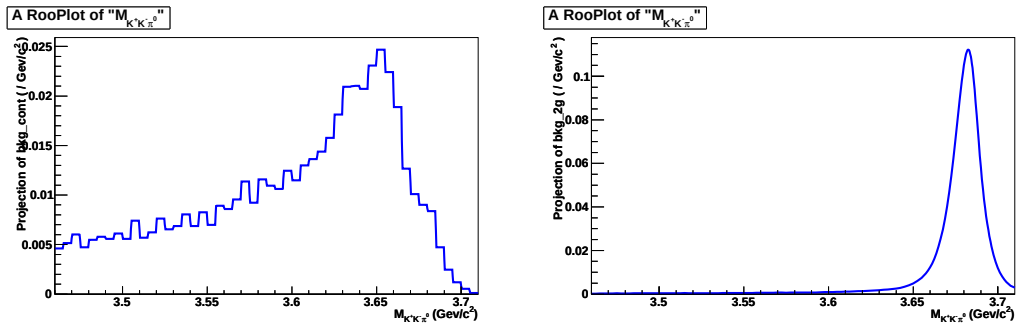

(a) mass spectrum of FSR events

(b) mass spectrum of noFSR events

Figure 7: Lineshape for $\pi^0 KK$. Considering the difference in simulation between data and MC, the ratio of FSR events and noFSR events will be fixed while fitting the final mass spectrum.

$$f_{FSR} = f_{DATA}/f_{MC} \tag{2}$$

While f_{FSR} stands for the difference in simulation between data and MC (f_{DATA} and f_{MC} express the respective FSR proportion of data and MC, and if the MC simulation is exactly right (describes data well), this $f_{FSR} \sim 1$. So, the deviation from 1 could stand for the difference in simulation between data and MC). From the analysis in $\psi(2S) \to \gamma\pi^+\pi^- K^+K^-$ and $\psi(2S) \to \gamma 2(\pi^+\pi^-)$ [6], $f_{FSR} = 1.39 \pm 0.08$ and $f_{FSR} = 1.70 \pm 0.10$ can be obtained respectively. Roughly, the f_{FSR} for $\gamma KK\pi^0$ should be

$$f_{FSR}^{\psi(2S)\to\gamma KK\pi 0} = \frac{f_{FSR}^{\psi(2S)\to\gamma\pi^+\pi^- K^+K^-}}{\sqrt{f_{FSR}^{\psi(2S)\to\gamma 2(\pi^+\pi^-)}}}, \tag{3}$$

By the way, the R_{FSR} factor will be fixed while fitting the final $K^+K^-\pi^0$ mass spectrum. And from the simulation, this kind of background contributes 7.0 ± 2.6 events in $\eta_c(2S)$ signal mass region $[3.6, 3.65]\mathrm{GeV/c^2}$.

4.4.2 Lineshape of $\pi^0\pi^0 KK$

The lineshape of $\pi^0\pi^0 KK$ background can be estimated by measuring those $\pi^0\pi^0 KK$ events in data and then scaling the measured mass spectrum to "$\gamma KK\pi^0$" final state.

With a similar event selection and a 6C kinematic fitting, the $\pi^0\pi^0 KK$ mass spectrum in data calculated as same as signal is shown in Fig. 8(a). According to the MC simulation of $\pi^0\pi^0 KK$, the efficiency ratio of these two event selections ($\pi^0\pi^0 KK$ and $\gamma KK\pi^0$) can be obtained as shown in Fig. 8(b). Finally, the $K^+K^-\pi^0$ mass spectrum of these $\pi^0\pi^0 KK$ events can be estimated by scaling the measured $\pi^0\pi^0 KK$ spectrum in data with the efficiency ratio spectrum as Fig. 9 shows.

In consideration of the unavoidable background of $\pi^0\pi^0 KK$ events coming from $\chi_{cJ(J=1,2)}$, we scale the corresponding mass spectrums of $\chi_{cJ(J=1,2)}$ in the same way. At last we fit the whole $\pi^0\pi^0 KK$ background mass spectrum with $\pi^0\pi^0 KK$ "signal" and $\chi_{cJ(J=1,2)}$ "background" to get the lineshape of $\pi^0\pi^0 KK$ as the red line shows (using single-Gaussian as PDF), which will be used to fit the final $K^+K^-\pi^0$ mass spectrum (contributes 2.2 ± 1.5 background events in the signal mass region). Incidentally, the used fitting number of this background is fixed just like the $\psi(2S) \to \omega KK$ background.

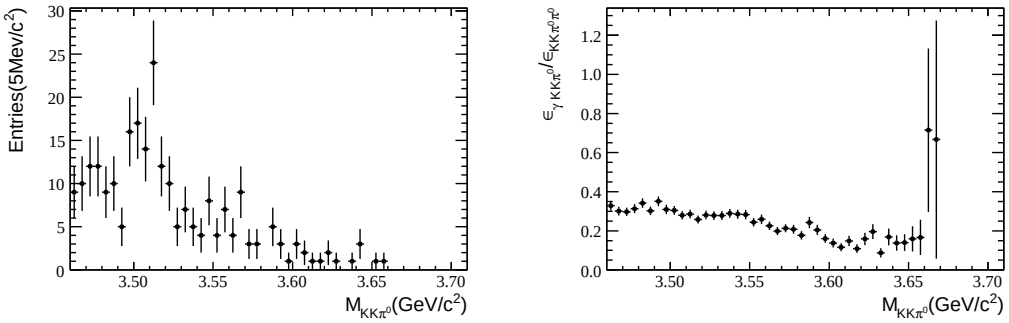

(a) final mass spectrum of $\pi^0\pi^0KK$ (b) scale factor from MC

Figure 8: Measurement of $\pi^0\pi^0KK$ background events. a) Mass spectrum of $\pi^0\pi^0KK$ background calculated as same as signal. b) Efficiency ratio of these two event selections ($\gamma KK\pi^0$) and $\pi^0\pi^0KK$.

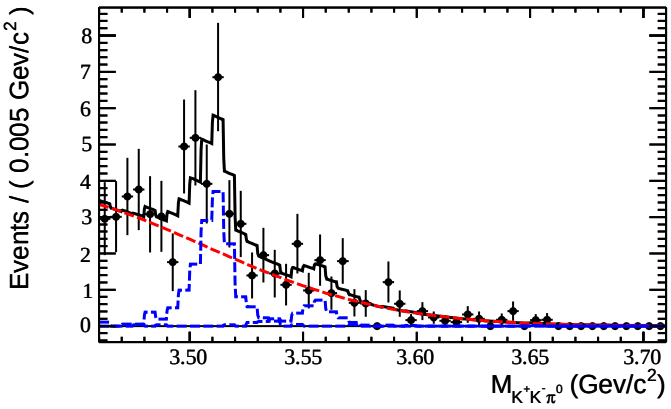

Figure 9: Lineshape of $\pi^0\pi^0KK$ background events. Blue histogram is $\chi_{cJ(J=1,2)}$ "background" and red is $\pi^0\pi^0KK$ "signal", which is used for final fitting as the lineshape of $\pi^0\pi^0KK$ background.

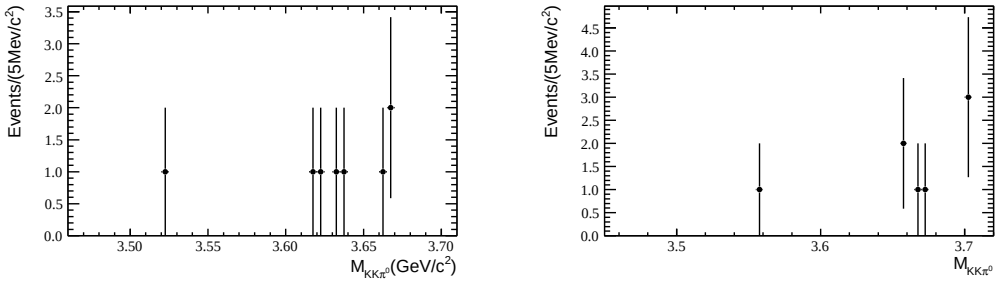

(a) original mass spectrum of continuum data (b) shifted mass spectrum of continuum data

Figure 10: Background of continuum. a) The original mass spectrum calculated from data collected at $\sqrt{s} = 3.65\mathrm{GeV/c^2}$. b) The shifted mass spectrum for the continuum contribution to $\sqrt{s} = 3.686\mathrm{GeV/c^2}$.

4.5 Background from continuum

The background from continuum can be estimated by the data sample taken at $\sqrt{s} = 3.65\mathrm{GeV/c^2}$. After the same selection, the mass spectrum for the continuum data is shown in Fig. 10(a). The scale factor for the whole mass spectrum is

$$f_{continuum} = \frac{156.4\ \mathrm{pb^{-1}}}{42.6\ \mathrm{pb^{-1}}} \cdot (\frac{3.65\ \mathrm{GeV}}{3.686\ \mathrm{GeV}})^2 = 3.6, \tag{4}$$

where $156.4\mathrm{pb^{-1}}$ and $42.6\mathrm{pb^{-1}}$ are the integrated luminosity at 3.686GeV and 3.65GeV respectively, $(\frac{3.65\ \mathrm{GeV}}{3.686\ \mathrm{GeV}})^2$ is for the cross section difference between the two energy points. Considering the energy difference, the mass is shifted according to the following operation:

$$m \to a(m - m_0) + m_0, \tag{5}$$

where $m_0 = 1.122\ \mathrm{GeV/c^2}$ is the mass threshold for $\pi^0 KK$ which should not be shifted, the coefficient $a = (3.686 - m_0)/(3.65 - m_0) = 1.014$ makes sure the events at $\sqrt{s} = 3.65\ \mathrm{GeV/c^2}$ are shifted to $\sqrt{s} = 3.686\ \mathrm{GeV/c^2}$. The shifted mass spectrum for the continuum contribution is shown in Fig. 10(b). And there is almost no continuum event exists in $\eta_c(2S)$ mass region, $[3.6, 3.65]\mathrm{GeV/c^2}$.

5 Fitting of mass spectrum

5.1 Monte Carlo estimation

With all these informations of background, we are able to carry out an estimation using the corresponding Monte Carlo samples (based on the known branching ratios of the respective decay channels in PDG). From the estimation shown in Fig. 11, we can see that the vicinity of $\eta_c(2S)$ signal region agrees with data well. What's more, according to the estimation (including the tail of $\chi_{cJ(J=1,2)}$, which contribute 4.8 ± 0.7 and 4.5 ± 1.1 events of "background" respectively), there should be 19 ± 4 background events expected in the blinded signal mass region $[3.6, 3.65]\mathrm{GeV/c^2}$, however, there are 47 ± 7 events founded in data sample in the same mass region, so, what are they?

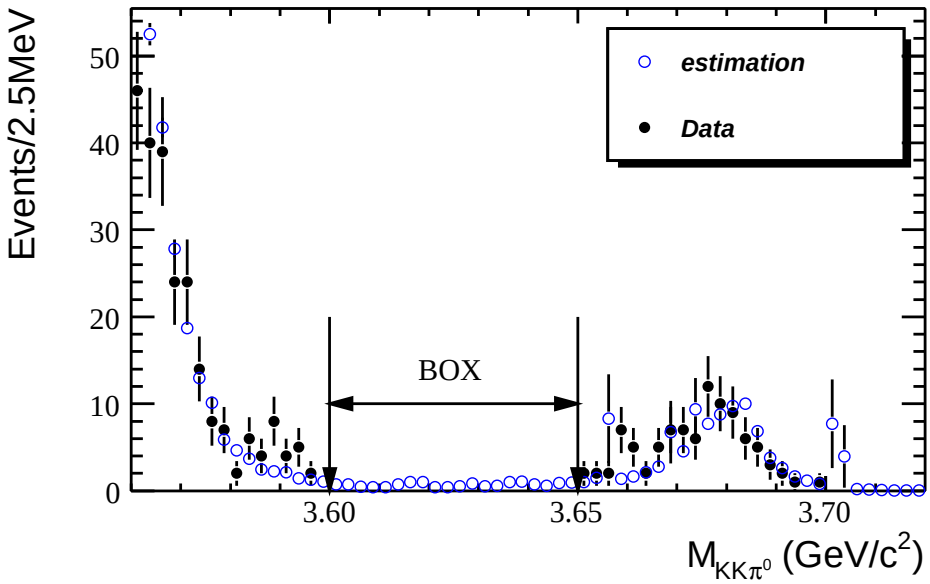

Figure 11: Invariant mass spectrum of $\pi^0 KK$ for events passing through the whole selection criteria. Black dots are data, and circles are MC simulation of all known backgrounds.

There is a significant difference in data sample comparing to the expected MC simulation in the signal mass region. This may imply something new in data. After opening the blinded mass region, a bump is observed on the mass spectrum as shown in Fig. 12.

5.2 Lineshape of signal

Before we fit the final mass spectrum, lineshapes of the three signal, $\chi_{cJ(J=1,2)}$ and $\eta_c(2S)$, will be described as follows:

- $\chi_{cJ(J=1,2)}$: Based on a reliable hypothesis that the main differences between MC simulation and real data are just the mass correction and the detector resolution, we just apply the $\pi^0 KK$ mass spectrum histogram of the corresponding $\chi_{cJ(J=1,2)}$ Monte Carlo samples convolved with a Gaussian resolution function as the PDF (Probability Distribution Function).

- $\eta_c(2S)$: The lineshape for $\eta_c(2S)$ should be described carefully as its width is not small (about 10 MeV) and the relative variation to E_γ is also large ($\sim 10MeV/50MeV$ 20%). A natural line shape for $\eta_c(2S)$ produced by such a M1 transition is given by

$$(E_\gamma^3 \times BW(m) \times damping(E_\gamma)) \otimes Gauss(0,\sigma), \tag{6}$$

where m is the invariant mass of $K^+K^-\pi^0$, $E_\gamma = \frac{m_{\psi'}^2 - m^2}{2m_{\psi'}}$ is the energy of the transition photon in the rest frame of ψ', $damping(E_\gamma)$ is the function to damp the diverging tail raised by E_γ^3 and $Gauss(0,\sigma)$ is the gaussian function describing the detector resolution. The possible form of the

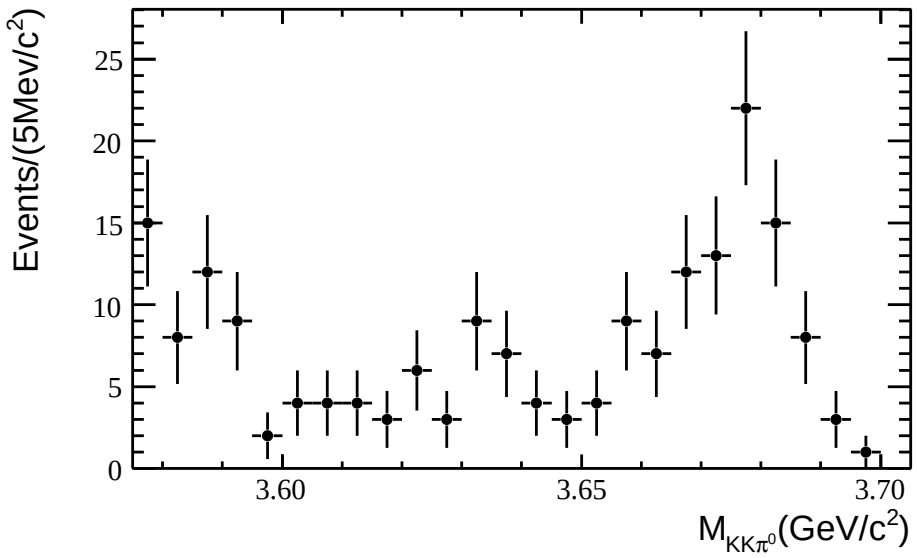

Figure 12: Opening the blind BOX of mass spectrum, a bump is found, and there should be something new in data sample.

damping function is somewhat arbitrary, and one suitable function used by KEDR for a similar process is [8]

$$\frac{E_0^2}{E_\gamma E_0 + (E_\gamma - E_0)^2}, \tag{7}$$

where $E_0 = \frac{m_{\psi'}^2 - m_{\eta_c(2S)}^2}{2m_{\psi'}}$ is the peaking energy of the transition photon. Another damping function used by CLEO [9] is inspired by the overlap of wave functions

$$\exp(-E_\gamma^2/8\beta^2), \tag{8}$$

with $\beta = (65.0 \pm 2.5)$MeV from CLEO's fit. This function (8) is criticized that it has no theoretical justification, which can also be signalled by the unnatural scale of β [10]. So in our analysis, the damping function (7) will be used in the fitting to give the final results, and the not-so-justified form (8) will be used to estimate the possible uncertainty caused by the form of damping functions.

5.3 Resolution of $\eta_c(2S)$

We study the mass resolution of $\chi_{cJ(J=1,2)}$ with the mass difference between the 4C kinematic fitted mass and the true mass from MC generation, which are shown in Fig. 13(a)−Fig. 13(c), and have a linear mass dependence with a small slope (Fig. 13(d)). So the mass resolution for $\eta_c(2S)$ is fixed to the linear extrapolation from the mass resolution of $\chi_{cJ(J=1,2)}$ signals in data sample.

5.4 Fitting of mass spectrum

Finally, a unbinned maximum likelihood method is used for fitting. With the recent measurements using two-photon processes from Babar [11], Belle [12] and the average from precious experiments [13], one

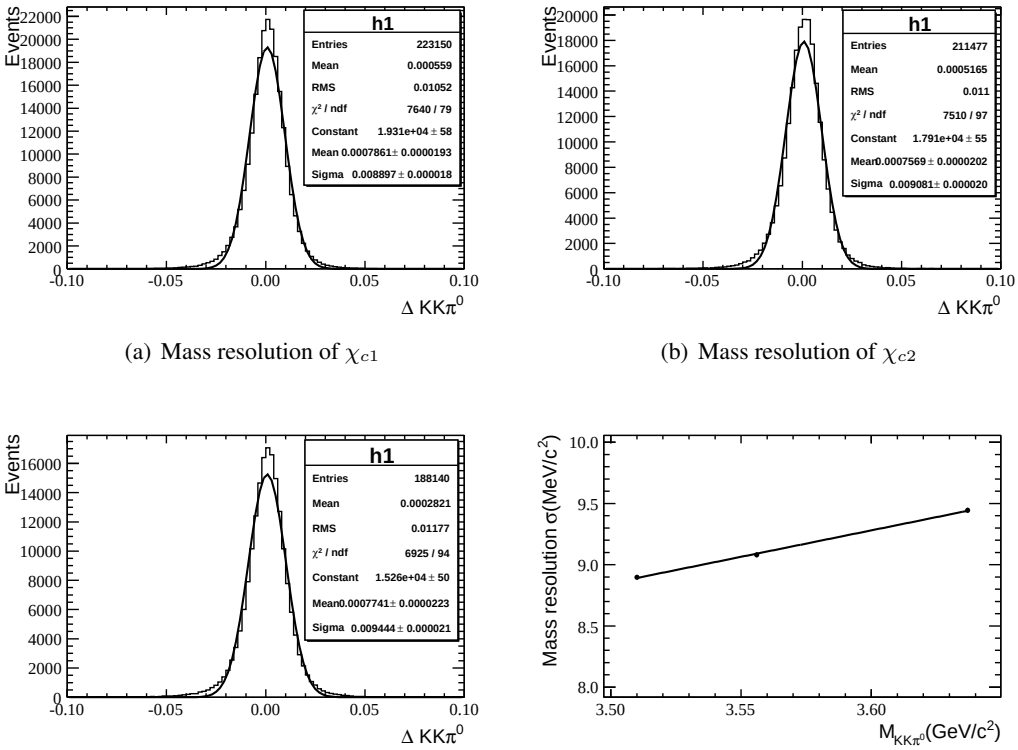

(a) Mass resolution of χ_{c1}

(b) Mass resolution of χ_{c2}

(c) Mass resolution of $\eta_c(2S)$

(d) Linear correlation for the mass resolution

Figure 13: Mass shift and resolution of $\chi_{cJ(J=1,2)}$ and $\eta_c(2S)$ with the mass difference between the 4C kinematic fitted mass and the true mass from MC generation. d) The linear correlation for the mass resolution of $\chi_{cJ(J=1,2)}$ and $\eta_c(2S)$ MC samples.

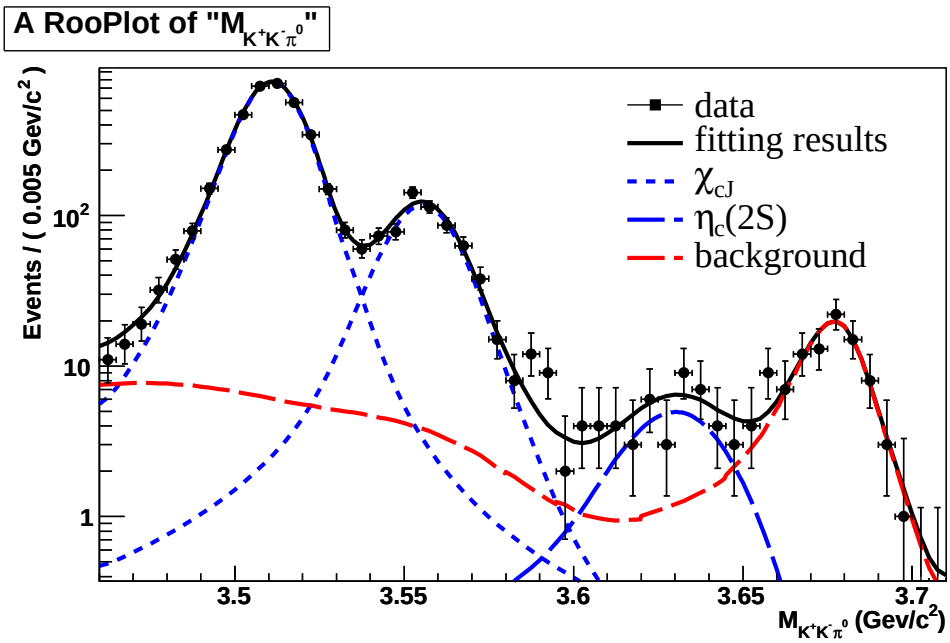

Figure 14: Maximum likelihood fitting of the mass spectrum

Table 2: Fitting results of the mass spectrum

details	results
$M_{\eta_c(2S)}$ (MeV/c^2)	3634.5±4.9
Width of $\eta_c(2S)$ (MeV)	10.4 ± 4.2 (10.4 fixed)
Number of events	39.8±8.5
Significance	5.8σ

can get the best average value for the width of $\eta_c(2S)$ to be 10.4 ± 4.2MeV. So finally, the width of $\eta_c(2S)$ is fixed to this best world average. The statistical significance of the $\eta_c(2S)$ signal is calculated from the difference between the likelihoods of the fitting with and without the signal $\eta_c(2S)$, which is about 5.8σ. Fig. 14 shows the fitting, and the fitting results are listed in Table 2.

5.5 Consistency checks

5.5.1 Number of signal between estimation and fitting

The estimated number of signal events is $N_{signal}^{estimation} = 47-19 = 28\pm8$ in the mass region [3.6,3.65]GeV/c^2, and the fitted number of signal events is $N_{signal}^{fitting} = 32 \pm 6$, so the difference between estimation and fitting is $\Delta N_{signal} = 4 \pm 10$, and is about one standard deviation, which is a good consistency check of the analysis.

5.5.2 Check on the corresponding branching ratios of χ_{cJ}

From the analysis, one can also get the measurements of the branching ratios for $\psi(2S) \to \gamma\chi_{cJ(J=1,2)}$, $\chi_{cJ(J=1,2)} \to K^+K^-\pi^0$. The results are summarized in Table 3, which also agree with PDG well.

Table 3: Consistency checks of branching ratios of $\psi(2S) \to \gamma\chi_{cJ(J=1,2)}$, $\chi_{cJ(J=1,2)} \to K^+K^-\pi^0$

	N_{obs}	ϵ	$\mathcal{B}(\psi' \to \gamma\chi_{cJ(J=1,2)}, \chi_{cJ(J=1,2)} \to K^+K^-\pi^0)$	$\mathcal{B}$ from PDG
χ_{c1}	3638 ± 62	22.3%	$(1.55 \pm 0.14) \times 10^{-4}$	$(1.77 \pm 0.26) \times 10^{-4}$
χ_{c2}	638 ± 29	21.1%	$(2.89 \pm 0.27) \times 10^{-5}$	$(2.91 \pm 0.76) \times 10^{-5}$

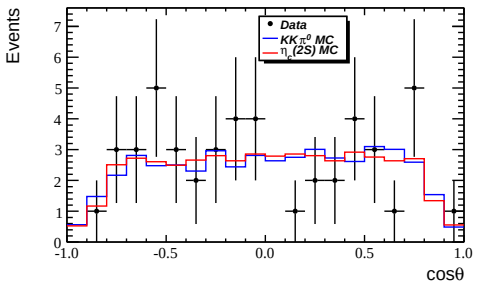

(a) polar angle

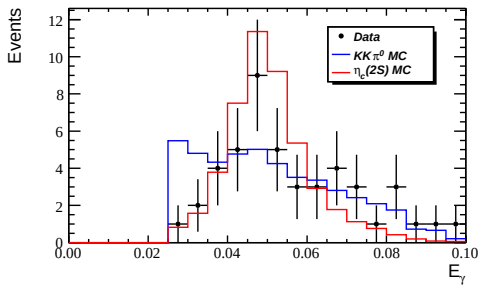

(b) corrected energy

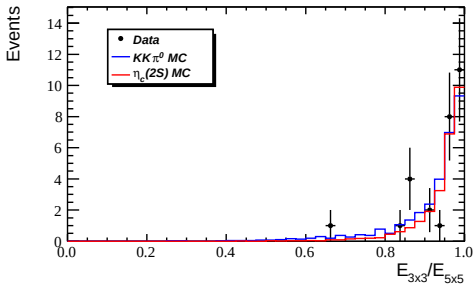

(c) energy component

Figure 15: Distribution of the selected transition photon within the signal mass region [3.6,3.65]GeV. a) polar angle distribution. b) corrected energy diatribution. c) energy component distribution.

5.5.3 Check on the selected transition photon

The distribution of polar angle, energy and E_{3*3}/E_{5*5} (the energy deposited in the $3*3$ crystals around the shower center over the one in the $5*5$ crystals) for the selected transition photon are shown in Fig. 15(a)-Fig. 15(c) (within signal mass region) as well as Fig. 16(a)-Fig. 16(c) (above signal mass region).

From the comparison, we could consider that behaviors of photons within the signal mass region [3.6,3.65]GeV are just consistent with real photons. However, those above 3.65GeV probably look like fake clusters in EMC as they have different distributions from signal.

6 Systematic uncertainties

The possible systematic uncertainties on the fitted mass and the number of events for $\eta_c(2S)$ are considered as following:

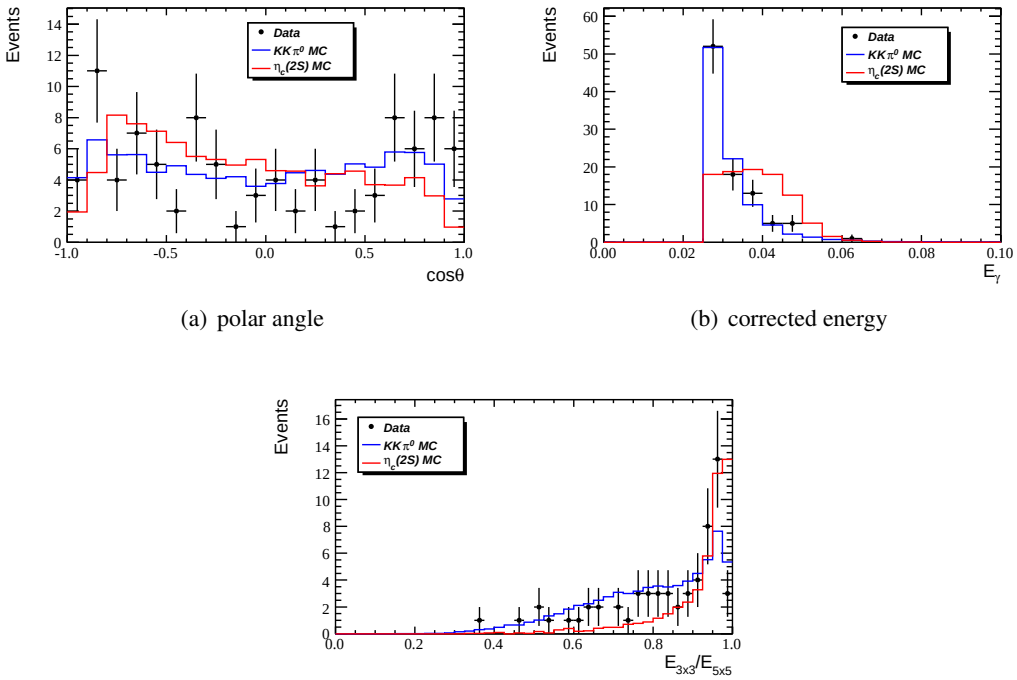

(a) polar angle

(b) corrected energy

(c) energy component

Figure 16: Distribution of the selected transition photon above the signal mass region [3.6,3.65]GeV. a) polar angle distribution. b) corrected energy diatribution. c) energy component distribution.

6.1 Tracking efficiency for Kaon

Refer to the analysis of $\psi(2S) \to \gamma\eta_c(2S)$, $\eta_c(2S) \to \gamma K_S^0 K\pi$ [7], the uncertainty of the tracking efficiency for Kaon is about 2% per track.

6.2 Photon reconstruction

The uncertainty due to photon detection and photon conversion is 1% per photon [5]. This is determined from studies of photon detection efficiencies in well understood decays such as $J/\psi \to \rho^0\pi^0$, $\rho^0 \to \pi^+\pi^-$, $\pi^0 \to \gamma\gamma$ and study of photon conversion via $e^+e^- \to \gamma\gamma$.

6.3 Particle identification

From the BESIII former analysis, the uncertainty of Particle ID is about 2% per particle.

6.4 Kinematic fitting

In order to evaluate the systematic uncertainty of the kinematic fitting, we choose $\psi(2S) \to \gamma\chi_{cJ(J=1,2)}$, $\chi_{cJ(J=1,2)} \to KK\pi^0$ events according to the following criteria (similar to signal event selection but without kinematic fitting):

- 2 charged tracks with net charge zero, and at least 3 good photons.
- charged tracks are fitted with common VertexFit package to IP.
- cycle all those good photons, whose difference between the total reconstructed 4-momentum of all the final state particles and that of the original $\psi(2S)$ is minimum are kept as the good photon candidates.
- Particle ID (same to the signal event selection).

As Fig. 17 shows, for the used requirement $\chi^2 < 30$, the selection efficiencies of data and MC are 0.87 and 0.91 respectively, as a result, the systematic uncertainty of the kinematic fitting is about $(0.91 - 0.87)/0.91 = 4.4\%$.

6.5 Total number of $\psi(2S)$ events

Based on the earlier analysis [1], this item should be about 4%.

6.6 Fixed ratio between FSR and noFSR events

Considering the worst siuation of the fixed ratio between FSR and noFSR events in dealing with the $\pi^0 KK$ background events, which is 0.15 ± 0.01, it will cause 1.1% systematic uncertainty for the fitted number of signal, and the corresponding uncertainty for the fitted mass is about 0.0MeV.

6.7 Fixed width of $\eta_c(2S)$

As showed above, the uncertainty of the fixed width of $\eta_c(2S)$ is about 4.2Mev (Table 2), and the caused effects are about 8.9% on the fitted number and 1.2MeV on the fitted mass.

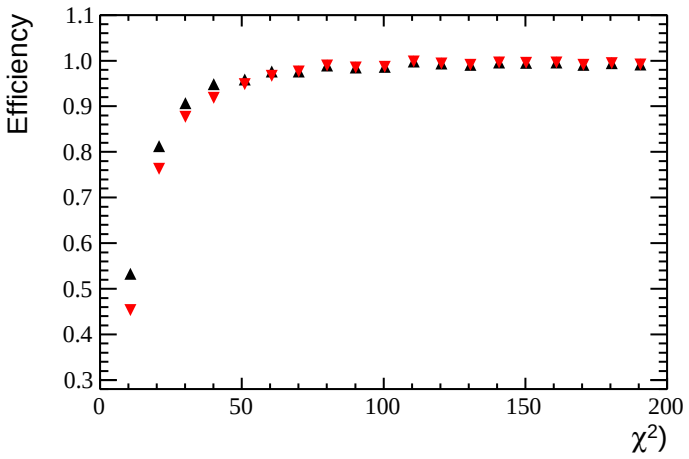

Figure 17: Systematic uncertainty of the kinematic fitting obtained from $\chi_{cJ(J=1,2)}$ analysis.

6.8 Fixed fitting Number of ωKK events

In view of the uncertainty of the fixed fitting number of ωKK background events (84 ± 24), we can obtain that it will cause about 1.0% systematic uncertainty on fitted number and 0.1MeV on mass.

6.9 Lineshape of ωKK background

To estimate the uncertainty caused by the lineshape of ωKK background, we apply directly the shape from Mento Carlo sample for the fitting (without parameterizations), and the systematic uncertainties are about 0.2% and 0.3MeV for fitted number and mass.

6.10 Fixed fitting Number and lineshape of $\pi^0\pi^0 KK$ background

This item is estimated similarly to the ωKK background, and the results are, respectively, for fixed amount, 1.5% on signal event number and 0.2MeV on mass, for the lineshape, 2.3% on signal event number and 0.3MeV on fitted mass.

6.11 Damping factor for $\eta_c(2S)$ signal lineshape

We use two different forms of damping factors for fitting (KEDR and $CLEO_c$), and take the difference between them as the uncertainty, which is about 22.1% for event number and 2.3MeV for main mass respectively.

6.12 Fitting mass region

As there are hardly events above 3.71GeV, we change the fitting mass region from [3.46,3.71]GeV to [3.45,3.71]GeV, and it doesn't influence the mass although causes about 0.9% on the fitted event number.

Table 4: Systematic uncertainties

Systematic Uncertainties	Event Number (%)	Fitted Mass (MeV)
Tracking efficiency	4	-
Photon reconstruction	3	-
Particle ID	4	-
Kinematic fitting	4.4	-
Number of $\psi(2S)$	4	-
Fixed ratio of FSR	1.1	0.0
Fixed width of $\eta_c(2S)$	8.9	1.2
Fixed number of ωKK	1.0	0.1
Lineshape of ωKK	0.2	0.3
Fixed number of $\pi^0\pi^0 KK$	1.5	0.2
Lineshape of $\pi^0\pi^0 KK$	2.3	0.3
Damping factor	22.1	2.3
Fitting mass range	0.9	0.0
$\eta_c(2S)$ decay dynamics	3.5	-
In total	25.8	2.6

6.13 $\eta_c(2S)$ decay dynamics

The decay $\eta_c(2S) \to KK\pi^0$ is treated as phase space in the standard signal MC. The recent result through $B^\pm \to K^\pm\eta_c(2S)$,$\eta_c(2S) \to K^0_S K^\pm\pi^\pm$ decays from Belle gave the Dalitz distribution of the 3-body $\eta_c(2S)$ decay, which was used to generate an alternative signal MC sample to estimate the efficiency of the decay with some intermediate states. Finally, a small difference about 3.5% was found between phase space MC and MC with intermediate states, which was taken as the systematic uncertainty duo to $\eta_c(2S)$ decay dynamics.

7 Results and discussion

7.1 Fitting results

From the fitting results of $\eta_c(2S)$, we could obtain the branching ratio for $\psi' \to \gamma\eta_c(2S), \eta_c(2S) \to K^+K^-\pi^0$ as:

$$\begin{aligned}\mathcal{B}(\psi' \to \gamma\eta_c(2S)) \times \mathcal{B}(\eta_c(2S) \to K^+K^-\pi^0) &= \frac{N_{\eta_c(2S)}}{\epsilon \cdot \mathcal{B}(\pi^0 \to \gamma+\gamma) \cdot N_{\psi'}} \\ &= \frac{39.8}{0.194 \times 0.988 \times (1.06 \times 10^8)} \\ &= (1.96 \pm 0.42) \times 10^{-6} \end{aligned} \quad (9)$$

where ϵ is the efficiency of the event selection from full simulation, $\mathcal{B}(\pi^0 \to \gamma+\gamma)$ is the branching ratio for $\pi^0 \to \gamma+\gamma$, and $N_{\psi'}$ is the total number of ψ'.

Table 4 showes the systematic uncertainties on the measured branching ratio and fitted mass of $\eta_c(2S)$.

So the final result of the measured branching ratio is $\mathcal{B}(\psi' \to \gamma\eta_c(2S)) \times \mathcal{B}(\eta_c(2S) \to K^+K^-\pi^0) = (1.96 \pm 0.42 \pm 0.51) \times 10^{-6}$, meanwhile, the fitted mass $M_{\eta_c(2S)} = 3634.5 \pm 4.9 \pm 2.6 MeV$. (The first

Table 5: Fitting results of $\psi' \to \gamma\eta_c(2S)$, $\eta_c(2S) \to K\bar{K}\pi$

Decay channel	$\gamma K^+K^-\pi^0$	$\gamma K^0_S K^\pm\pi^\mp$
Observable	$39.8 \pm 8.5 \pm 10.2$	$71.8 \pm 10.7 \pm 12.9$
$M_{\eta_c(2S)}$ (MeV/c^2)	3634.5$\pm$4.9 $\pm$ 2.6	3636.1 $\pm$ 2.0 $\pm$ 1.2
Branch ratio (E-6)	$1.96 \pm 0.42 \pm 0.51$	$4.06 \pm 0.61 \pm 0.73$
Significance	5.8σ	6.5σ

uncertainty is statistic, and the second one is systematic.)

7.2 Summary

Using the largest $\psi(2S)$ data sample in the world which was collected by BESIII, we searched for the M1 transition between $\psi(2S)$ and $\eta_c(2S)$ through the hadronic final states $\eta_c(2S) \to K\bar{K}\pi$ ($K^0_S K^\pm\pi^\mp$ and $K^+K^-\pi^0$). Actually, this is the first observation of the M1 transition between $\psi(2S)$ and $\eta_c(2S)$. And the measured results are listed in Table 5.

From the comparison of two decay channels, it can be found that the Isospin Symmetry is well kept within experimental uncertainties. By the way, the systematic uncertainty is just dominated by the fixed width of $\eta_c(2S)$ as well as the maybe arbitrary damping factor.

References

[1] G. LI and Z.Y. WANG, BESIII note (2010).

[2] M.Ablikim *et al.* (BES Collaboration), Phys. Lett. B 614, 37 (2005).

[3] Zhu Kai, talk at DQ/Validation Meeting (2010)

[4] Ye Chen, Jiaxu Zuo, talk at DQ/Validation Meeting on 18 January (2010)

[5] M.Ablikim *et al.* (BESIII Collaboration), Phys. Rev. D 81, 052005 (2010).

[6] Y.Q. WANG, talk "Search for new $\eta_c(2S)$ decays" at the BESIII Collaboration 2010 Fall Meeting.

[7] L.L. WANG, talk "Search for new $\eta_c(2S)$ decays" at the BESIII Collaboration 2010 Fall Meeting.

[8] V.V. Anashin *et al.*, arXiv:1012.1694 [hep-ex]

[9] R. E. Mitchell *et al.* (CLEO Collaboration), Phys. Rev. Lett. 102, 011801 (2009).

[10] N. Brambilla, P. Roig and A. Vairo, arXiv:1012.0773v1 [hep-ph] 3 Dec 2010.

[11] V. Druzhinin (for BaBar Collaboration), talk "Recent results on two-photon physics at BaBar" at ICHEP 2010.

[12] H. Nakazawa (for Belle Collaboration), talk "Particle production in two-photon collisions at Belle" at ICHEP 2010.

[13] K. Nakamura et al., Journal of Physics G 37, 075021 (2010).

[14] B. Aubert *et al.* (Babar Collaboration), Phys. Rev. D 78, 012006 (2008)